# Experimental Demonstration of Reconfigurable "Digital Average" of Two 20-Gbaud Phase-Encoded Data Channels Using Nonlinear Optical Wave Mixing

**Amir Minoofar[1]*, Hao Song[1], Ahmed Almaiman[2], Narek Karapetyan[1], Wing Ko[1], Kaiheng Zou[1], Huibin Zhou[1], Muralekrishnan Ramakrishnan[1], Murale Annavaram[1], Jonathan L. Habif[1,3], Moshe Tur[4], and Alan E. Willner[1,5]**

1. Depart. of Electrical Engineering, University of Southern California, Los Angeles, CA 90089, USA. Email: minoofar@usc.edu
2. King Saud University, Riyadh, Saudi Arabia
3. University of Southern California, Information Sciences Institute, 890 Winter St., Waltham, MA 02451, USA
4. School of Electrical Engineering, Tel Aviv University, Ramat Aviv 69978, ISRAEL
5. Dornsife Depart. of Physics & Astronomy, University of Southern California, Los Angeles, CA 90089, USA

**Abstract:** We experimentally demonstrate the reconfigurable "digital average" of two 10/20-Gbaud phase-encoded data channels using two nonlinear optical stages. In the first nonlinear stage, we compute the average. In the second nonlinear stage, we multicast the average result to the input signals wavelengths.

## 1. Introduction

Several functions performed in electronic digital signal processing (DSP) units can be significant bottlenecks at high data rates and for several data channels [1]. An example of one such function that can limit DSP performance is to perform "digital average" [2,3]. This average performed on parallel "digital bits", is not simply a single mean value from a set of multiple amplitudes [4]. For example, the digital average of two binary streams "111" and "011" is "101". Such digital average is important in various DSP functions used in communication systems (e.g., suppressing nonlinear interactions) or computer science applications (e.g., federated learning) [5-7].

The above potential bottleneck may often occur when transmitting high-speed data streams from different nodes in a processing network. The interconnection medium may well be across an optical communication system in which the data is encoded in amplitude and/or phase of the optical carrier wave [8,9]. Therefore, there may be benefits to performing the digital average in the optical domain instead of the electronic domain since optics: (a) may be faster than electronics due to the ability to operate on multiple parameters of the optical wave, (b) may be fast enough to operate at the line rate and not time demultiplex as is common in electronics, (c) may have the potential for tunability and reconfigurability in data rate and format, and (d) can help avoid inefficient optical-to-electrical-to-optical conversion if the data originates in the optical domain [10-12]. Although there have been many publications about achieving various DSP functions using optical signal processing (OSP), to our knowledge we are not aware of any high-speed OSP approach to achieve a "digital average" [1, 10-11].

In this paper, we experimentally demonstrate a reconfigurable "digital average" system for two 10/20-Gbaud phase-encoded data channels using nonlinear optical wave mixing in two nonlinear optical stages. We compute the average in a highly nonlinear fiber (HNLF) as the first nonlinear stage. In the second stage, we multicast the generated digital average to the initial wavelengths of the two input data channels using a periodically poled lithium niobate (PPLN) waveguide. The measured phase of the output bitstream verifies the concept of the proposed "digital average" system. The final result (i.e., after multicasting the average result) shows error vector magnitudes (EVMs) performance of ~ 18-21%.

## 2. Concept

Figure 1 shows the concept of the OSP system for computing the "digital average" of two phase-encoded signals. Generally, to perform the function of digital average, there are two arithmetical operations to be performed: the division and the summation, which are shown in Fig. 1(a). Thus, the flow of our proposed "digital average" system is as follows: (i) we start with bitstream $A$ and bitstream $B$ which are coming from two different users, each carrying a 2-bit number (0,1,2,3) that are mapped in the four distinct phases as $\varphi_A$ or $\varphi_B$=$(0, \pi/2, \pi, 3\pi/2)$ of a quadrature-phase-shift-keying (QPSK) phase diagram; (ii) we perform the division on these phase-encoded data, such that the phase levels become $\varphi_A/2$ or $\varphi_B/2$=$(0, \pi/4, \pi/2, 3\pi/4)$ and the input data information is encoded as a 4-phase-shift-keying (4-PSK) modulation format, wherein constellation points occupy the top half of the phase diagram. The optical wave of inputs within one symbol duration can be expressed as $E_A = a\,.exp(j(2\pi f_A t + \varphi_A/2))$ and $E_B = b\,.exp(j(2\pi f_B t + \varphi_B/2))$, where $f_A$ or $f_B$ are the carrier frequencies; (iii) we perform the addition of the halved input phases in a summation stage and obtain an optical wave as $E_R = ab\,.exp(j(2\pi f_R t + \varphi_R))$, where $\varphi_R$=$(\varphi_A + \varphi_B)/2$. Thus, the constellation points occupy seven distinct phase levels of $(0, \pi/4, \pi/2, \ldots, 5\pi/4, 3\pi/2)$ in an 8-PSK data format, and the average result would be a 3-bit number; and (iv) we multicast the output of the digital average system to the wavelengths of the initial input signals.

In Fig. 1(b1), we show the mapping of an input bitstream with 2-bit numbers where the phases are mapped to four phase levels. Figure (b2) shows the mapping of the output bitstream with a 3-bit number where the phases are mapped to seven phase levels for our proposed digital average system. Finally, Fig. 1(b3) shows the corresponding number of the digital average result based on the input numbers. This scheme mimics a processing network in which two users are initially located at different locations, where they can send their data to a central processing node to perform the desired function [2,7]. By multicasting the computed average result, the users can use it for their next round of processing.

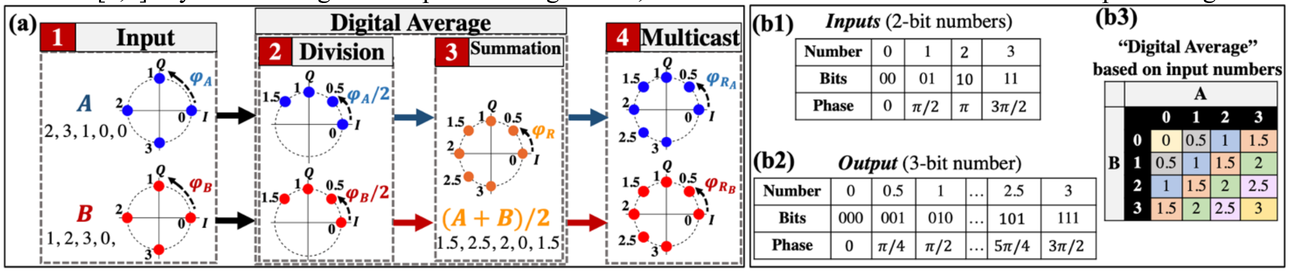


Figure 1. (a) Concept of computing the digital average of two phase-encoded signals. The figure consists of four parts as: (1) input phase-encoded data channels, in which a 2-bit number (0,1,2,3) represented in a QPSK data format is fed to the system; (2) division, in which the input phases are halved to be $(0, \pi/4, \pi/2, 3\pi/4)$; (3) summation, in which the halved phases are summed that results in another phase-encoded signal having seven phase levels of $(0, \pi/4, \pi/2, \ldots, 5\pi/4, 3\pi/2)$; and (4) multicast, in which the average result is multicast to the input signal wavelengths. (b1-2) Corresponding bits and phase levels for the input and output numbers. (b3) The digital average result as a 3-bit number (0,0.5,1,…, 3) based on the two input numbers (0,1,2,3).

## 3. Experimental Setup

We verify the concept by performing (i) the division by loading the phase-divided signal directly to an electro-optic modulator, and (ii) the summation using wave mixing in an HNLF. Moreover, at the end of the digital average system, we multicast the output to wavelengths of the input signals in a PPLN waveguide. Figures 2(a-b) show the experimental setup and principle for demonstrating the reconfigurable "digital average" of two phase-encoded signals using nonlinear optical wave mixing. Five tunable laser sources at $\lambda_A$=1549.32 nm, $\lambda_B$=1550.12 nm, $\lambda_P$=$\lambda_{P_B}$=1552.52 nm, $\lambda_{P_A}$=1553.32 nm, and $\lambda_{P_C}$=1555.72 nm are used. Using an arbitrary waveform generator (AWG) and an in-phase and quadrature (IQ) modulator, both laser sources at $\lambda_A$ and $\lambda_B$ are modulated with a 10/20 Gbaud 4-PSK data format. The two 4-PSK data signals are then separated by a wavelength demultiplexer. We use (i) a 2-m single mode fiber to decorrelate the data channels, and (ii) a variable optical delay line to minimize the symbol time skew between two data channels. The two phase-encoded data channels together with a CW pump at $\lambda_P$ are launched into an HNLF, having a length of 520 m, a zero-dispersion wavelength (ZDW) of ~1555 nm, and a nonlinear coefficient of 20 $W^{-1}\cdot km^{-1}$. Consequently, through a non-degenerate four-wave mixing (FWM) process, the average result ($R$) is generated at $\lambda_R$ = 1546.92 nm.

To multicast the computed result into $\lambda_A$ and $\lambda_B$, the generated average of the first stage is filtered, amplified, and coupled with three other separate laser sources. Then, the four waves are used as inputs to the PPLN waveguide. In both nonlinear stages, a polarization controller (PC) is used for each of the input optical signals that are fed to the optical nonlinear element to align the state of polarization of interacting signals and maximize the conversion efficiency of wave mixing. Through cascaded (i) sum frequency generation (SFG) between the optical waves $R$ and $P_C$ located symmetric with respect to the quasi-phase-matching (QPM) of the PPLN waveguide and (ii) difference frequency generation (DFG) with the two other dummy pumps $P_A$ and $P_B$, the result is multicast to $\lambda_A$ and $\lambda_B$ as well. To ensure that the wavelengths of the input data channels and the multicasting results are similar, (i) the wavelength of dummy pumps $P_A$ and $P_C$ are tuned, and (ii) the QPM wavelength of the PPLN is temperature tuned to 1551.3 nm using a thermo-electric cooler. Finally, a coherent receiver is used for data recovery and decoding of different phase levels of the output signal.

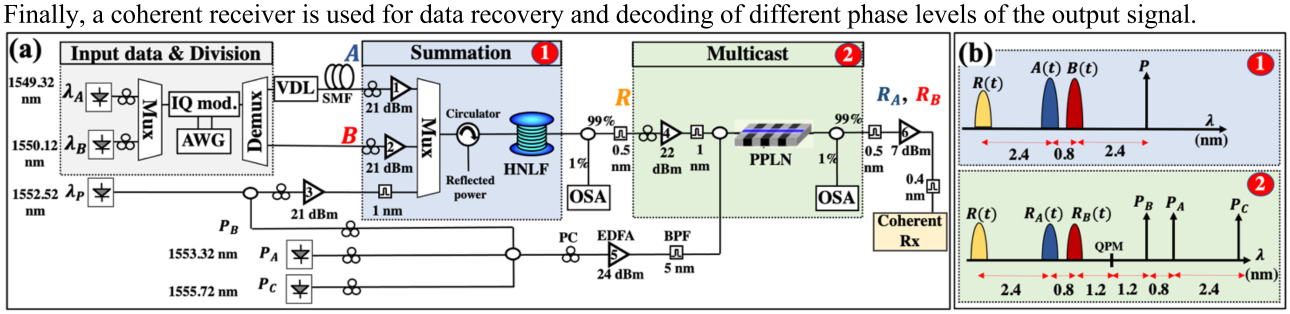


Figure 2. (a) Experimental setup and (b) principle of performing the digital average of two 10/20-Gbaud phase-encoded signals using nonlinear optical wave mixing in two nonlinear optical stages. In the first stage, using a highly nonlinear fiber (HNLF), the average result of the two phase-encoded signals ($A$ and $B$) will be computed. In the second stage, using a periodically poled lithium niobate (PPLN) waveguide, the computed result ($R$) is multicast to the input signal wavelengths (i.e., generating $R_A$ at $\lambda_A$ and $R_B$ at $\lambda_B$). AWG: arbitrary waveform generator; IQ Mod.: in-phase & quadrature modulator; VDL: variable delay line; SMF: single mode fiber; PC: polarization controller; EDFA: erbium-doped fiber amplifier; BPF: band-pass filter; OSA: optical spectrum analyzer; QPM: quasi-phase-matching.

## 4. Results and Discussion

Figure 3 shows the experimental result of the "digital average" of both 10 and 20-Gbaud phase-encoded signals. The constellation diagrams for each signal at the first stage ($A$, $B$, $R$) and second stage ($R_A$, $R_B$) are shown in Fig. 3(a1-3) for 10/20 Gbaud data rates. As can be seen from the corresponding EVM values, the EVM of the final result ($R_A$, $R_B$ ~ 19-

21%) is higher compared with the average result ($R$ ~ 12-14%) or the inputs ($A$, $B$ ~ 9-11%). This could be due to the accumulated phase noise of each input when performing nonlinear wave mixing in each stage.

The measured optical spectrum of the (i) HNLF output and (ii) PPLN output using an optical spectrum analyzer (OSA) are shown in Figs. 3(b1-2) for the 20-Gbaud data rate. The first spectrum shows that due to the FWM of the three input waves (i.e., two input data channels $A$ and $B$, and the dummy pump $P$) multiple mixing terms (including the average result $R$ at $\lambda_R$ = 1546.92 nm) will be generated at the output of the HNLF. The measured input optical power to the HNLF is ~ 21 dBm. At higher input optical power to the HNLF, the EVM value increases (e.g., at 22 dBm the EVM of $R$ is ~ 22%), which might be due to increased undesired nonlinearity effects in the HNLF that distort the generated signal [13]. By measuring the difference in power level ($\Delta_1$) between inputs ($A, B$) and the average result ($R$), the conversion efficiency is estimated to be ~ -17.2 dB. The measured input optical power to the PPLN waveguide is ~ 24 dBm. By estimating the power difference ($\Delta_2$) between $R$ and $R_A/R_B$, the conversion efficiency of wave mixing in the second stage is ~ -24.2 dB. The lower conversion efficiency of PPLN might be because the two input signals involved in the SFG process are ~ 4.4 nm apart, far from the QPM due to specified wavelengths of the data channels [14].

To verify the digital average of two phase-encoded signals, the phase levels of the two input data channels ($A$ and $B$) and the average result (i.e., $R$=$(A+B)/2$) are captured. The results of recovered phase levels and their corresponding numbers are shown in Fig. 3(c), where 14 symbols were captured in 700 ps. The average result ($R$) confirms that the digital average of input data channels is achieved using nonlinear wave mixing.

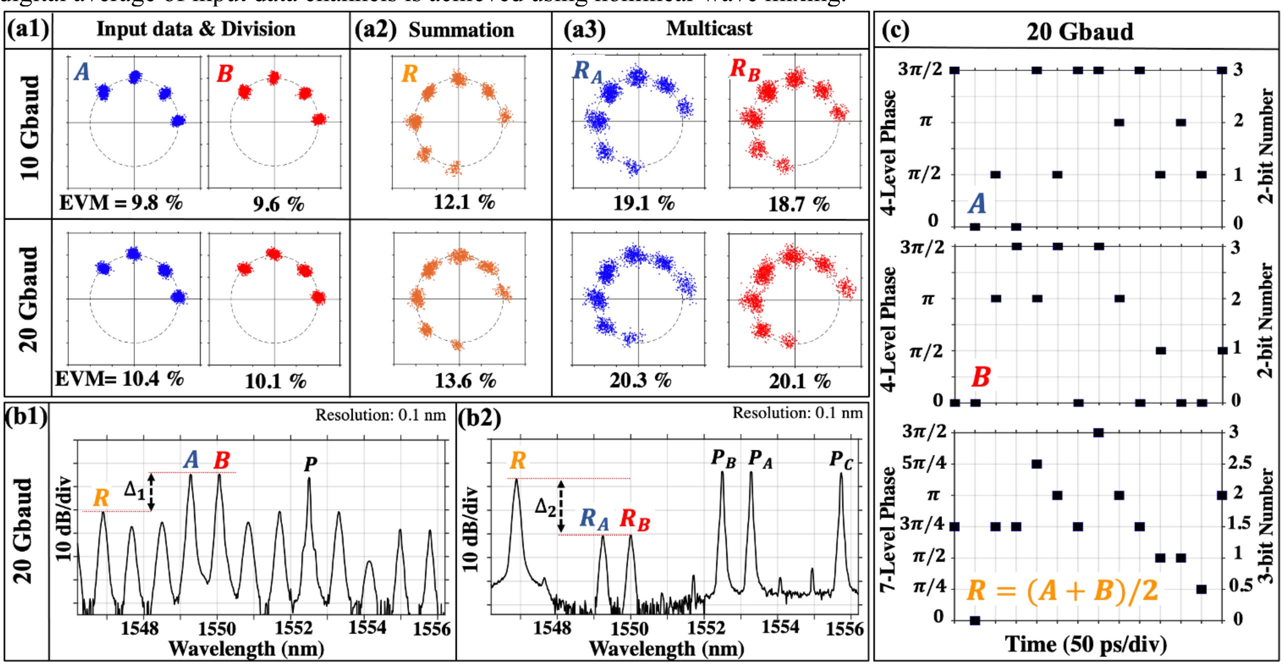


Figure 3. (a1-3) Constellation diagrams with their corresponding EVM values for $A$, $B$, $R$, $R_A$, and $R_B$. (b1-2) Output optical spectrum of the HNLF (to sum) and PPLN (to multicast), respectively. The conversion efficiency of each stage is measured by the difference in the optical power levels and labeled as $\Delta_1$ and $\Delta_2$. (c) Captured 4-level phases of the two 20-Gbaud data channels as inputs (2-bit numbers) and 7-level phases of the digital average as the output (a 3-bit number) in 700 ps.

It should be noted that this approach could be potentially scaled in terms of (i) the number of bits by using higher-order phase-encoded signals (e.g., using 8-PSK data channels as the input represents a 3-bit number), and (ii) the number of input data channels by cascading multiple nonlinear stages, wherein each of them performs the digital average for only two of the input data channels. Moreover, it might also be possible to have the input data already on the optical wave and halve the phase of the input data format using some all-optical phase-sensitive approach [13].

## Acknowledgment

Support of DARPA under award number HR001120C0088; Qualcomm Innovation Fellowship (QIF).

## References

[1] H. Zhou et al., Light: Sci. & Appl. 11(1), no. 30, (2022).
[2] H. Wang et al., arXiv:2002.06440, (2020).
[3] J. Gao et al., IEEE Internet Computing, 12(6), 37, (2008).
[4] E. A. Clancy et al., IEEE Trans. Biomed. Eng., 41(2), 159, (1994).
[5] X. Liu et al., Nature Photon., 7(7), 560 (2013).
[6] H. Fujisaka et al., IEEE Proc. Circ. Dev. Sys. 149(3), 159 (2002).
[7] J. Konecny et al., arXiv:1610.05492v2, (2017).
[8] J. Zhao et al., Appl. Sci., 9(19), 4192 (2019).
[9] K.-P. Ho, New York:Springer-Verlag, (2005).
[10] P. Minzioni et al., J. of Optics, 21, 063001 (2019).
[11] V. Bangari et al., IEEE JSTQE, 26(1), 7701213 (2020).
[12] J. Capmany et al., J. Lightw. Technol., 31(4), 571 (2013).
[13] R. Slavik et al., Nature Photon., 4, 690 (2010).
[14] C. Langrock et al., J. Lightw. Technol., 24(7), 25 (2006).